PHOTONICS Research

Noise-sidebands-free and ultra-low-RIN 1.5 μm single-frequency fiber laser towards coherent optical detection

Qilai Zhao,[1] Zhitao Zhang,[1] Bo Wu,[2] Tianyi Tan,[1] Changsheng Yang,[1,3] Jiulin Gan,[1] Huihui Cheng,[1] Zhouming Feng,[1] Mingying Peng,[1] Zhongmin Yang,[1,4,5] and Shanhui Xu[1,3,*]

[1]State Key Laboratory of Luminescent Materials and Devices and Institute of Optical Communication Materials, South China University of Technology, Guangzhou 510640, China
[2]College of Optoelectronic Technology, Chengdu University of Information Technology, Chengdu 610225, China
[3]Guangdong Engineering Technology Research and Development Center of High-Performance Fiber Laser Techniques and Equipments, Zhuhai 519031, China
[4]Guangdong Engineering Technology Research and Development Center of Special Optical Fiber Materials and Devices, Guangzhou 510640, China
[5]Guangdong Provincial Key Laboratory of Fiber Laser Materials and Applied Techniques, South China University of Technology, Guangzhou 510640, China
*Corresponding author: flxshy@scut.edu.cn

Received 18 December 2017; revised 4 February 2018; accepted 6 February 2018; posted 6 February 2018 (Doc. ID 317939); published 27 March 2018

A noise-sidebands-free and ultra-low relative intensity noise (RIN) 1.5 μm single-frequency fiber laser is demonstrated for the first time to our best knowledge. Utilizing a self-injection locking framework and a booster optical amplifier, the noise sidebands with relative amplitudes as high as 20 dB are completely suppressed. The RIN is remarkably reduced by more than 64 dB at the relaxation oscillation peak to retain below −150 dB/Hz in a frequency range from 75 kHz to 50 MHz, while the quantum noise limit is −152.9 dB/Hz. Furthermore, a laser linewidth narrower than 600 Hz, a polarization-extinction ratio of more than 23 dB, and an optical signal-to-noise ratio of more than 73 dB are acquired simultaneously. This noise-sidebands-free and ultra-low-RIN single-frequency fiber laser is highly competitive in advanced coherent light detection fields including coherent Doppler wind lidar, high-speed coherent optical communication, and precise absolute distance coherent measurement.

OCIS codes: (140.3510) Lasers, fiber; (140.3570) Lasers, single-mode; (270.2500) Fluctuations, relaxations, and noise.

https://doi.org/10.1364/PRJ.6.000326

1. INTRODUCTION

In recent years, single-frequency fiber lasers have been extensively studied because of some advantages such as high beam quality, all-fiber configuration, and narrow linewidth, which enable them to be extensively applied in various fields, including nonlinear frequency conversion, high-precision spectroscopy, coherent beam combing, and laser detection [1–4]. As a result, coherent optical detection is becoming one of the primary techniques of laser detection, benefitting from many prominent characteristics such as high signal-to-noise ratio (SNR), high conversion gain, and reducible signal light information [5,6]. However, the SNR and measuring precision of coherent optical detection are critically limited by the existence of serious noise sidebands as well as the disturbance of intrinsic relative intensity noise (RIN), especially in coherent Doppler wind lidar, high-speed coherent optical communication, precise absolute distance coherent measurement, and other advanced coherent optical detection applications [7–9]. Therefore simultaneous suppression of both noise sidebands and RIN of a single-frequency fiber laser, which can significantly enhance the sensitivity and SNR of coherent light detection systems, becomes a crucial task.

In coherent light detection based on single-frequency fiber lasers, it can be found that two noise peaks exist on both sides of the detected signal [10]. The noise peaks are called noise sidebands. The presence of noise sidebands limits the measurement results and the minimum detectable signals in coherent light detection [11,12]. For single-frequency fiber lasers, previous theoretical research has briefly reported that RIN and frequency noise at the relaxation oscillation frequency f_r will usually lead to sidebands in the optical spectrum at $\nu = \nu_0 \pm f_r$, where ν_0 is the laser central frequency [13].

However, despite existing theoretical analysis, relevant experimental demonstration is surprisingly lacking. Furthermore, to date, the optimization of the noise sidebands in single-frequency fiber lasers has never been revealed, either.

With regard to RIN, even if a well-designed continuous wave (CW) free-running laser may be sufficiently stable for most applications, amplitude stabilization is still required to achieve the high performance required in a coherent detection system, which is conducive to distinguish weak signal from a complex radio-frequency spectrum [14,15]. Regarding RIN suppression, a common technology is the optoelectronic feedback method, while the suppressed amplitude and bandwidth are restricted by the natural inferior property of the optoelectronic feedback loop [16]. Another technique to reduce RIN is based on a mode-cleaner with feedback loop [17]. Nevertheless, the mode-cleaner, suffering from environmental sensitivity and voluminous architecture [18], increases the operation difficulty and causes mismatch between the spatial light structure and the all-fiber configuration of the single-frequency fiber laser.

Recently, we have presented broad-bandwidth near-shot-noise-limited intensity noise suppression of a single-frequency fiber laser based on a semiconductor optical amplifier with optoelectronic feedback [19]. In this paper, we introduce a noise-sidebands-free and ultra-low-RIN 1.5 μm linearly polarized single-frequency fiber laser. With the comprehensive effect of a self-injection locking (SIL) system and a booster optical amplifier (BOA), not only are the noise sidebands with relative amplitudes of 20 dB completely suppressed, but the RIN is also reduced to below −150 dB/Hz in a wide frequency range, which approaches the quantum noise limit. Moreover, the linewidth is compressed to narrower than 600 Hz. It is believed that this single-frequency fiber laser can effectively enhance the sensitivity and SNR of coherent light detection applications. Taking coherent Doppler wind lidar for example, a complete suppression of the noise sidebands contributes to an available detection of the Doppler small-frequency-shift signal, which corresponds to a detection of low wind speed [10]. Near-quantum-noise-limited performance is conducive to distinguish weak signal from a complex frequency spectrum, which can evidently reduce the complexity of back-end detection systems [12]. In addition, <600 Hz laser linewidth is quite beneficial in optical remote sensing and meteorology [14].

2. EXPERIMENTAL SETUP

The experimental setup of the noise-sidebands-free and ultra-low-RIN 1.5 μm single-frequency fiber laser based on BOA and SIL is displayed in Fig. 1(c), and the two other structures of BOA only and SIL only are shown in Figs. 1(a) and 1(b) for comparison. The laser cavity is formed by a 1.3 cm highly Er^{3+}/Yb^{3+} co-doped phosphate fiber with a pair of fiber Bragg gratings [20]. The rare earth ions are doped uniformly in the core region with concentrations of 3.0 mol.% for Er^{3+}, and 5.0 mol.% for Yb^{3+}, respectively. The absorption of the phosphate fiber is 7.9 dB/cm @ 980 nm. The polarization-maintaining (PM) narrow-band fiber Bragg grating has a peak reflectivity of 60% and a 3 dB bandwidth of 0.06 nm, while that of the broadband fiber Bragg grating

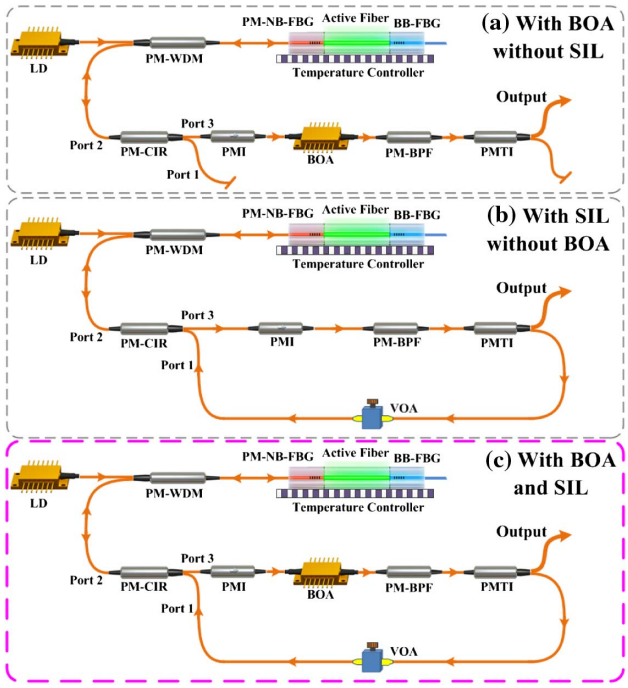

Fig. 1. Experimental setup in different structures (a) with BOA without SIL, (b) with SIL without BOA, and (c) with BOA and SIL. FBG, fiber Bragg grating; PM-NB-FBG, PM narrow-band FBG; BB-FBG, broadband FBG; LD, laser diode; PM-WDM, PM wavelength division multiplexer; PM-CIR, PM circulator; PMI, PM isolator; PM-BPF, PM bandpass filter; PMTI, PM tap isolator; VOA, variable optical attenuator.

is >99.95% with a 3 dB bandwidth of 0.35 nm. The physical lengths of the fiber Bragg gratings are both 1.5 cm.

The laser cavity is temperature-controlled through a cooling system with a resolution of 0.05°C, and it is pumped via a 980 nm single-mode laser diode with a PM wavelength division multiplexer. The laser from the PM wavelength division multiplexer is then launched into port 2 of a PM circulator. Port 3 of the PM circulator and the input port of a BOA are connected by a PM isolator, which is used to guarantee unidirectional transmission of the laser. The BOA is a high saturation output power, high bandwidth, low-ripples, and PM optical amplifier, with a central wavelength of 1550 nm, a 3 dB gain bandwidth of 85 nm, a saturation output power of 15 dBm, and a small signal gain of 27 dB. It incorporates a highly efficient InP/InGaAsP quantum well layer structure and a reliable ridge waveguide design. A designed PM bandpass filter (3 dB bandwidth: 1 nm) is added to filter out the amplified spontaneous emission brought in by the BOA. Then a 10/90 PM tap isolator, combining a PM tap coupler and a polarization-sensitive isolator into a single compact package, is employed to split 10% of the laser power through a variable optical attenuator launching into the port 1 of the PM circulator, which renewedly enters the laser cavity to realize the SIL. The 90% port of the PM tap isolator is the final laser output. All the experimental optical paths are well fixed on the optical table with special optical glue to reduce the unnecessary acoustic vibrations from the external environment.

During the experiment, the driving current of the laser diode is 250 mA, corresponding to the 14 mW laser output power. The laser power feeding into the BOA is 12 mW, while the driving current of the BOA is set to 200 mA. The power injected to the PM circulator is adjusted to 1 mW by the variable optical attenuator. Ultimately, the output power from the 90% port of the PM tap isolator is 13 mW.

The measurement scheme of coherent light detection is based on a Mach–Zehnder interferometer. A 30/70 optical coupler splits the output laser into two beams. The 30% beam is frequency shifted by an acousto-optic modulator, while the 70% beam is time delayed by a delay fiber. Then a 50/50 optical coupler combines two laser beams launching into a high-speed photodetector to acquire the detected signal.

3. RESULTS AND DISCUSSION

In the experiment, various technologies, i.e., BOA only, SIL only, and BOA combined with SIL, are investigated with respect to the RIN suppression and noise sidebands elimination. The resultant RINs in different frequency ranges are compared with the quantum noise limit as shown in Fig. 2. To ensure consistency, the laser power is attenuated to 0.5 mW before being launched into an InGaAs photodetector with a bandwidth of 150 MHz, and the corresponding quantum noise limit is −152.9 dB/Hz. For the laser passing through the BOA only, the RIN is reduced by about 20 dB in a frequency range from 0 to 5 MHz, and it approaches −150 dB/Hz at frequency greater than 10 MHz. When the laser carries out the SIL operation without BOA, the relaxation oscillation peak is reduced by 28 dB from −86 dB/Hz to −114 dB/Hz.

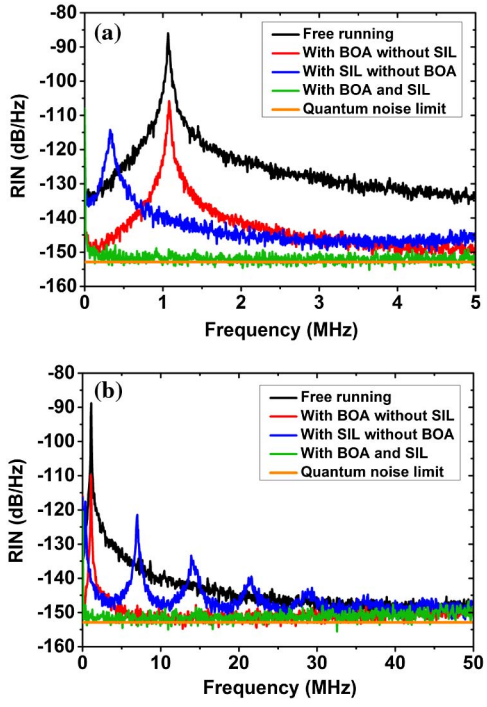

Fig. 2. RIN spectra of this single-frequency fiber laser with different conditions. The quantum noise limit of −152.9 dB/Hz is also shown for comparison. (a) 0 to 5 MHz. (b) 0 to 50 MHz.

Further, the relaxation oscillation frequency is shifted to a low-frequency stage from 1.066 MHz to 328 kHz, which is due to the increase of the photon lifetime by the introduction of the SIL loop [21]. Unfortunately, a series of gradually weakened harmonic peaks with frequency spaces of 7.33 MHz arise in the RIN spectra, which are attributed to the recursion dynamics of the laser in the SIL laser system [22].

Significantly, with the comprehensive effect of BOA and SIL, the RIN peak is remarkably reduced by more than 64 dB from −86 to −150 dB/Hz, and the entire relaxation oscillation peak is eliminated. Meanwhile, the addition of BOA into the SIL scheme has effectively restrained the series of harmonic peaks. Therefore, based on the evolutionary dynamics process, it can be summarized that the BOA in the SIL system periodically suppresses the RIN in every circulation of the injecting signal. Ultimately, the RIN of the final output laser is controlled to be below −150 dB/Hz in a frequency range from 75 kHz to 50 MHz, which means the difference between the acquired RIN and the quantum noise limit is less than 3 dB. Besides, all these RIN spectra exhibit slow rises in the frequency range of more than 20 MHz, which result from the noise floor of the InGaAs photodetector.

Utilizing the single-frequency fiber laser with different statuses, the signals of coherent light detection are measured seriatim as shown in Fig. 3. During the free-running stage, two noise sidebands are observed in the coherent detected signal. The relative amplitudes of noise sidebands (RANS), defined as the amplitude differences between the peaks of the noise sideband and the signal floor, are more than 20 dB. The frequency spaces between the detected signal and these noise sidebands are 1.07 MHz. After injecting the output laser to the BOA, the RANS has increased by 5 dB to 25 dB. Meanwhile, the envelopes of these noise sidebands broaden to some extent. The origin of this phenomenon is attributed to the nonlinear dynamics from BOA, including the gain saturation mechanism and the self-modulation effect [23,24]. It indicates that the simple passing of BOA is difficult to suppress the noise sidebands in spite of its favorable performance in decreasing the RIN.

Interestingly, with the SIL scheme, a maximum RANS suppression of more than 20 dB is realized, and two noise sidebands are absolutely reduced. The reasons for this action in the SIL laser are twofold. First, the resultant increasing photon lifetime reduces the RIN level [25]. The photon lifetime, which

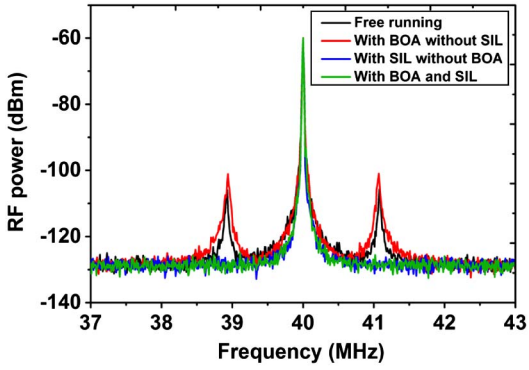

Fig. 3. Measured signals of coherent light detection of this single-frequency fiber laser in different statuses.

is the time needed for the light field to travel back and forth across the whole cavity, is extended by the introduction of the SIL loop [21]. Second, the SIL system drives a strong lasing frequency pulling, which causes the threshold gain difference of each mode [26]. This effect can promote the laser energy to concentrate on the main laser signal, and reduce the amplitude of the noise sidebands. Benefitting from the above two properties, only the main signal of the coherent detection exists.

Similarly, the coherent detected signal of the single-frequency fiber laser with SIL and BOA is also measured. The signal curve is almost coincident with that in the SIL scheme without BOA, and these noise sidebands also disappear. This indicates that the admirable performance of the coherent signal is not deteriorated by the insertion of the BOA in the SIL laser, thereby unveiling the unique advantage of the SIL technique in controlling the noise sidebands.

An optical spectrum with high optical SNR contributes to reducing the noise floor of the coherent detected signal. So the optical spectra are recorded at different output ports with a scanning span of 50 nm and a resolution bandwidth of 0.02 nm. To avoid a deterioration of optical SNR caused by the BOA-induced amplified spontaneous emission, a PM bandpass filter is employed, and the filtered spectrum is exhibited in Fig. 4(a). The amplified spontaneous emission is obviously filtered, as the optical SNR of the filtered signal is even higher than that of the free-running laser. In addition, the optical spectrum of the fiber laser with SIL is almost coincident with that without SIL, indicating that the spectral feather is not affected by the SIL loop. Eventually, the acquired optical SNR is larger than 73.0 dB. The polarization state of the final output laser is investigated, as shown in the inset of Fig. 4(a). A good linear polarization characteristic is demonstrated by virtue of the red dot located on the equator of the Poincaré sphere. The degree of polarization is measured to be 99.55%, corresponding to a more than 23 dB polarization-extinction ratio. This linearly polarized laser is conducive to improving the signal amplitude in coherent optical detection.

A single-longitudinal-mode working of the laser source is a basic requirement of coherent optical detection. Thus, the single-longitudinal-mode characteristic of this fiber laser after BOA with SIL is tested by a scanning Fabry–Perot interferometer with a resolution of 7.5 MHz and a free spectral range of 1.5 GHz. From Fig. 4(b), it can be seen that this fiber laser operated in single-longitudinal-mode status without mode-hop and mode competition phenomena.

The linewidth of the laser source is also momentous in coherent optical detection, especially for long-distance applications. The linewidths are evaluated by the self-heterodyne method involving a 48.8 km fiber delayed Mach–Zehnder interferometer and a 40 MHz fiber coupled acoustic optical modulator. Figure 5(a) shows the second-order self-heterodyne spectra of this single-frequency fiber laser with different conditions. It can be found that the simple addition of BOA does not change the linewidth, which is the same as that of a free-running single-frequency fiber laser. The linewidth of the

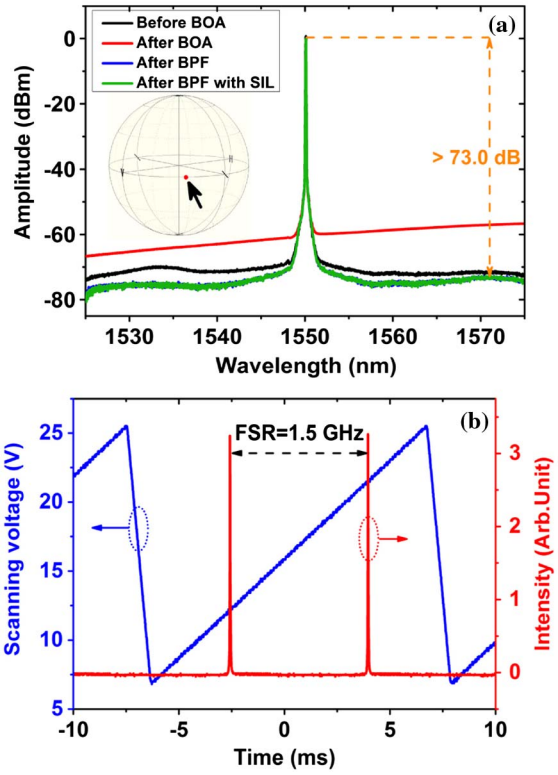

Fig. 4. (a) Optical spectra of this fiber laser at different output ports. The inset shows the degree of polarization of the final laser output (red dot) represented by a Poincaré sphere. (b) Measured single-longitudinal-mode characteristic of the final laser output.

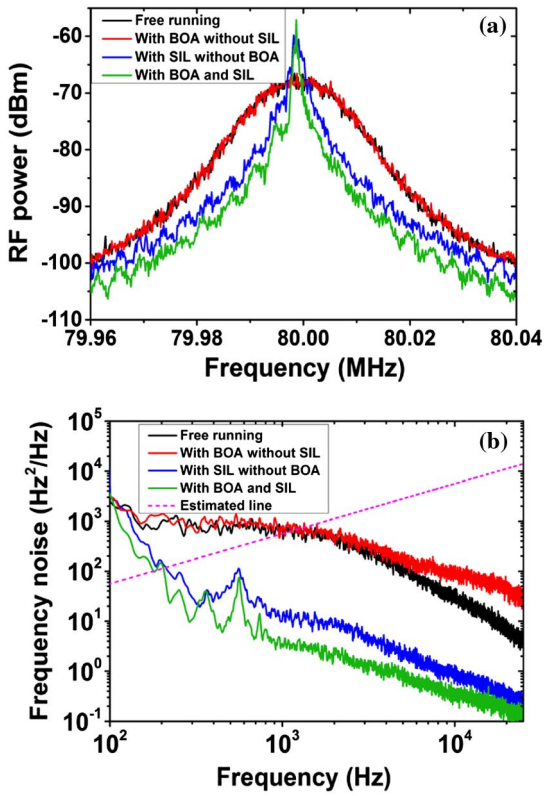

Fig. 5. (a) Measured self-heterodyne spectra of this fiber laser with different conditions. (b) Measured frequency noise spectra and estimation line for evaluation of linewidth.

free-running fiber laser is 2.2 kHz, and it is decreased to 0.87 kHz when SIL is adopted. For the single-frequency fiber laser with BOA and SIL, the self-heterodyne spectrum further narrows and the linewidth is about 0.58 kHz. The appearance of coherent envelopes indicates that the linewidth is smaller than the resolution of the measured system.

To overcome the limitation of the self-heterodyne method and obtain a more accurate laser linewidth, the frequency noise spectra are measured via a fiber Michelson interferometer with 100 m optical path difference and an optical phase demodulator [27]. Figure 5(b) shows the measured frequency noise spectra and the estimated line, from which we can calculate the laser linewidths to be 2.2, 2.3, 0.69, and 0.52 kHz, respectively [28]. Therefore, the laser linewidth in the final output is narrower than 0.6 kHz. In addition, the noise spikes at lower frequencies are attributed to the environmental disturbance, and the increase of frequency noise during the introduction of BOA results from its self-modulation effect [29].

4. CONCLUTIONS

We present a noise-sidebands-free and ultra-low-RIN 1.5 μm single-frequency fiber laser for the first time to our best knowledge. By means of the SIL technique combined with a BOA, the RANS is reduced by more than 20 dB and the noise sidebands are completely suppressed. A maximum reducing amplitude over 64 dB of the RIN is obtained, and the RIN is dramatically suppressed to be below −150 dB/Hz in the frequency range from 75 kHz to 50 MHz, while the quantum noise limit is −152.9 dB/Hz. Furthermore, the laser linewidth is effectively suppressed from 2.2 kHz to below 600 Hz. The polarization-extinction ratio and optical SNR are more than 23 and 73 dB, respectively. It is believed that the present finding not only constructively improves the application value of single-frequency fiber lasers in the sophisticated field but also effectively enhances the measured sensitivity and SNR of coherent light detection applications such as coherent Doppler wind lidar, high-speed coherent optical communication, and precise absolute distance measurement.

Funding. National Natural Science Foundation of China (NSFC) (11674103, 61535014, 61635004); Major Program of the National Natural Science Foundation of China (61790582); Fundamental Research Funds for Central Universities (2015ZM091, 2017BQ002); China National Funds for Distinguished Young Scientists (61325024); Natural Science Foundation of Guangdong Province (2016A030310410, 2017A030310007); Science and Technology Project of Guangdong (2014B050505007, 2015B090926010, 2016B090925004, 2017B090911005).

REFERENCES

1. S. W. Chiow, T. Kovachy, J. M. Hogan, and M. A. Kasevich, "Generation of 43 W of quasi-continuous 780 nm laser light via high-efficiency, single-pass frequency doubling in periodically poled lithium niobate crystals," Opt. Lett. **37**, 3861–3863 (2012).
2. T. Wu, X. Peng, W. Gong, Y. Zhan, Z. Lin, B. Luo, and H. Guo, "Observation and optimization of ^{4}He atomic polarization spectroscopy," Opt. Lett. **38**, 986–988 (2013).
3. P. Zhou, Y. Ma, X. Wang, H. Ma, X. Xu, and Z. Liu, "Coherent beam combination of three two-tone fiber amplifiers using stochastic parallel gradient descent algorithm," Opt. Lett. **34**, 2939–2941 (2009).
4. J. Geng, C. Spiegelberg, and S. Jiang, "Narrow linewidth fiber laser for 100-km optical frequency domain reflectometry," IEEE Photon. Technol. Lett. **17**, 1827–1829 (2005).
5. F. Peng, H. Wu, X.-H. Jia, Y.-J. Rao, Z.-N. Wang, and Z.-P. Peng, "Ultra-long high-sensitivity Φ-OTDR for high spatial resolution intrusion detection of pipelines," Opt. Express **22**, 13804–13810 (2014).
6. S. Kameyama, T. Ando, K. Asaka, Y. Hirano, and S. Wadaka, "Compact all-fiber pulsed coherent Doppler lidar system for wind sensing," Appl. Opt. **46**, 1953–1962 (2007).
7. C. J. Karlsson, F. Å. A. Olsson, D. Letalick, and M. Harris, "All-fiber multifunction continuous-wave coherent laser radar at 1.55 μm for range, speed, vibration, and wind measurements," Appl. Opt. **39**, 3716–3726 (2000).
8. G. Li, "Recent advances in coherent optical communication," Adv. Opt. Photon. **1**, 279–307 (2009).
9. I. Coddington, W. C. Swann, L. Nenadovic, and N. R. Newbury, "Rapid and precise absolute distance measurements at long range," Nat. Photonics **3**, 351–356 (2009).
10. P. Lindelöw, "*Fiber based coherent lidars for remote wind sensing*," Ph.D. dissertation (Technical University of Denmark, 2007).
11. G. A. Cranch, M. A. Englund, and C. K. Kirkendal, "Intensity noise characteristics of erbium-doped distributed feedback lasers," IEEE J. Quantum Electron. **39**, 1579–1586 (2003).
12. C. F. Abari, A. T. Pedersen, and J. Mann, "An all-fiber image-reject homodyne coherent Doppler wind lidar," Opt. Express **22**, 25880–25894 (2014).
13. E. Rønnekleiv, "Frequency and intensity noise of single frequency fiber Bragg grating lasers," Opt. Fiber Technol. **7**, 206–235 (2001).
14. J. P. Cariou, B. Augere, and M. Valla, "Laser source requirements for coherent lidars based on fiber technology," C. R. Physique **7**, 213–223 (2006).
15. P. Laporta, M. Marano, L. Pallaro, and S. Taccheo, "Amplitude and frequency stabilisation of a Tm–Ho:YAG laser for coherent lidar applications at 2.1 μm," Opt. Laser. Eng. **37**, 447–457 (2002).
16. S. Valling, B. Ståhlberg, and Å. M. Lindberg, "Tunable feedback loop for suppression of relaxation oscillations in a diode-pumped Nd:YVO_4 laser," Opt. Laser Technol. **39**, 82–85 (2007).
17. B. Willke, "Stabilized lasers for advanced gravitational wave detectors," Laser Photon. Rev. **4**, 780–794 (2010).
18. P. J. Barriga, C. Zhao, and D. G. Blair, "Astigmatism compensation in mode-cleaner cavities for the next generation of gravitational wave interferometric detectors," Phys. Lett. A **340**, 1–6 (2005).
19. Q. Zhao, S. Xu, K. Zhou, C. Yang, C. Li, Z. Feng, M. Peng, H. Deng, and Z. Yang, "Broad-bandwidth near-shot-noise-limited intensity noise suppression of a single-frequency fiber laser," Opt. Lett. **41**, 1333–1335 (2016).
20. S. H. Xu, Z. M. Yang, T. Liu, W. N. Zhang, Z. M. Feng, Q. Y. Zhang, and Z. H. Jiang, "An efficient compact 300 mW narrow-linewidth single frequency fiber laser at 1.5 μm," Opt. Express **18**, 1249–1254 (2010).
21. X. Huang, Q. Zhao, W. Lin, C. Li, C. Yang, S. Mo, Z. Feng, H. Deng, Z. Yang, and S. Xu, "Linewidth suppression mechanism of self-injection locked single-frequency fiber laser," Opt. Express **24**, 18907–18916 (2016).
22. C. Li, S. Xu, X. Huang, Y. Xiao, Z. Feng, C. Yang, K. Zhou, W. Lin, J. Gan, and Z. Yang, "All-optical frequency and intensity noise suppression of single-frequency fiber laser," Opt. Lett. **40**, 1964–1967 (2015).
23. U.-S. Lee, H.-D. Jung, and S.-K. Han, "Optical single sideband signal generation using phase modulation of semiconductor optical amplifier," IEEE Photon. Technol. Lett. **16**, 1373–1375 (2004).
24. H. Jiang, H. Wen, X. Zheng, Z. Liu, K. Wang, H. Zhang, and Y. Guo, "Improved optical single-sideband generation using the self-modulation birefringence difference in semiconductor optical amplifiers," Opt. Lett. **32**, 2580–2582 (2007).

25. S. Mo, X. Huang, S. Xu, Z. Feng, C. Li, C. Yang, and Z. Yang, "Compact slow-light single-frequency fiber laser at 1550 nm," Appl. Phys. Express **8**, 082703 (2015).
26. K. Hsu and S. Yamashita, "Single-polarization generation in fiber Fabry-Perot laser by self-injection locking in short feedback cavity," J. Lightwave Technol. **19**, 520–526 (2001).
27. Q. Zhao, Y. Zhang, W. Lin, Z. Wu, C. Li, C. Yang, Y. Zhang, Z. Feng, M. Peng, H. Deng, Z. Yang, and S. Xu, "Frequency noise of distributed Bragg reflector single-frequency fiber laser," Opt. Express **25**, 12601–12610 (2017).
28. G. D. Domenico, S. Schilt, and P. Thomann, "Simple approach to the relation between laser frequency noise and laser line shape," Appl. Opt. **49**, 4801–4807 (2010).
29. M. Yamada, "Analysis of intensity and frequency noises in semiconductor optical amplifier," IEEE J. Quantum Electron. **48**, 980–990 (2012).